THE JOURNAL OF BIOLOGICAL CHEMISTRY VOL. 286, NO. 11, pp. 9787–9796, March 18, 2011

Parathyroid Hormone-responsive Smad3-related Factor, Tmem119, Promotes Osteoblast Differentiation and Interacts with the Bone Morphogenetic Protein-Runx2 Pathway*

Received for publication, August 26, 2010, and in revised form, December 21, 2010 Published, JBC Papers in Press, January 14, 2011, DOI 10.1074/jbc.M110.179127

Itoko Hisa[‡], Yoshifumi Inoue[‡], Geoffrey N. Hendy[§], Lucie Canaff[§1], Riko Kitazawa[¶], Sohei Kitazawa[¶], Toshihisa Komori[‖], Toshitsugu Sugimoto[**], Susumu Seino[‡ ‡‡], and Hiroshi Kaji[‡ ‡‡2]

*From the [‡]Division of Diabetes and Endocrinology, Department of Internal Medicine, Kobe University Graduate School of Medicine, Kobe 650-0017, Japan, the [§]Departments of Medicine, Physiology, and Human Genetics, McGill University, and the Calcium Research Laboratory and the Hormones and Cancer Research Unit, Royal Victoria Hospital, Montréal, Québec H3A 1A1, Canada, the [¶]Division of Diagnostic Molecular Pathology, Kobe University Graduate School of Medicine, Kobe 650-0017, Japan, the [‖]Department of Cell Biology, Unit of Basic Medical Sciences, Nagasaki University Graduate School of Biomedical Sciences, Nagasaki, Japan, the **Department of Internal Medicine 1, Shimane University Faculty of Medicine, Izumo, Japan, and the [‡‡]Division of Cellular and Molecular Medicine, Department of Physiology and Cellular Biology, Kobe University Graduate School of Medicine, Kobe 650-0017, Japan*

The mechanisms whereby the parathyroid hormone (PTH) exerts its anabolic action on bone are incompletely understood. We previously showed that inhibition of ERK1/2 enhanced Smad3-induced bone anabolic action in osteoblasts. These findings suggested the hypothesis that changes in gene expression associated with the altered Smad3-induced signaling brought about by an ERK1/2 inhibitor would identify novel bone anabolic factors in osteoblasts. We therefore performed a comparative DNA microarray analysis between empty vector-transfected mouse osteoblastic MC3T3-E1 cells and PD98059-treated stable Smad3-overexpressing MC3T3-E1 cells. Among the novel factors, Tmem119 was selected on the basis of its rapid induction by PTH independent of later increases in endogenous TGF-β. The levels of Tmem119 increased with time in cultures of MC3T3-E1 cells and mouse mesenchymal ST-2 cells committed to the osteoblast lineage by BMP-2. PTH stimulated Tmem119 levels within 1 h as determined by Western blot analysis and immunocytochemistry in MC3T3-E1 cells. MC3T3-E1 cells stably overexpressing Tmem119 exhibited elevated levels of Runx2, osteocalcin, alkaline phosphatase, and β-catenin, whereas Tmem119 augmented BMP-2-induced Runx2 levels in mesenchymal cells. Tmem119 interacted with Runx2, Smad1, and Smad5 in C2C12 cells. In conclusion, we identified a Smad3-related factor, Tmem119, that is induced by PTH and promotes differentiation in mouse osteoblastic cells. Tmem119 is an important molecule in the pathway downstream of PTH and Smad3 signaling in osteoblasts.

Bone remodeling is controlled by bone resorption and subsequent osteoblastic bone formation. Insights into the mechanisms of osteoclastic bone resorption have led to the development of reagents that potently suppress bone resorption for the treatment of osteoporosis. On the other hand, the impairment of osteoblastic bone formation is considered to be the main driving force in age-related, glucocorticoid-induced, and diabetes-related osteoporosis. However, many aspects of osteoblastic bone formation remain to be understood. Intermittent parathyroid hormone (PTH)[3] is one of the most potent anabolic agents; it stimulates *de novo* osteoblastic bone formation and is superior to bisphosphonates in the treatment of osteoporosis (1, 2). The anabolic action of PTH is exerted partly through local growth factors and transcriptional regulators as well by as an anti-apoptotic action in osteoblasts (3, 4). However, the precise mechanisms by which PTH exerts its anabolic action on bone are incompletely understood.

We showed previously that Smad3, a crucial TGF-β-signaling molecule, promotes alkaline phosphatase (ALP) activity in mouse osteoblastic MC3T3-E1 cells (5, 6), and Borton *et al.* (7) have found that mice with targeted disruption of Smad3 exhibit osteopenia caused by decreased bone formation, suggesting that the Smad3 molecule is a promoter of bone formation. Moreover, we demonstrated that TGF-β-responsive ERK1/2 and c-Jun N-terminal kinase (JNK) cascades negatively regulate Smad3-induced transcriptional activity and ALP activity in osteoblasts (8). In that study, an inhibition of ERK1/2 enhanced Smad3-induced ALP activity in MC3T3-E1 cells.

On the other hand, we demonstrated that PTH rapidly enhances Smad3 expression in osteoblasts and that the PTH-Smad3 axis exerts anti-apoptotic effects in osteoblasts (9). Moreover, we showed that PTH stimulates osteoblast β-catenin levels via Smad3 (10, 11). In that study, PTH

* This work was supported by a grant from Mitsui Life Social Welfare Foundation (to H. K.), Grants-in-aid 17590961 and 21591179 from the Ministry of Science, Education, and Culture of Japan (to H. K.), the Global COE Program F11 from the Ministry of Education, Culture, Sports, Science, and Technology of Japan, and Canadian Institutes of Health Research Grant MOP-9315 (to G. N. H.).

[1] Supported by a Kidney Foundation of Canada Biomedical Fellowship and a fellowship from the Research Institute of the McGill University Health Centre.

[2] To whom correspondence should be addressed: Kobe University Graduate School of Medicine, 7-5-2 Kusunoki-cho, Chuo-ku, Kobe 650-0017, Japan. Tel.: 81-78-382-5861; Fax: 81-78-382-2080; E-mail: hiroshik@med.kobe-u.ac.jp.

[3] The abbreviations used are: PTH, parathyroid hormone; PTHrP, PTH-related protein; ALP, alkaline phosphatase; PMA, phorbol 12-myristate 13-acetate; Bt_2cAMP, N^6,$O^{2'}$-dibutyryl cyclic AMP; $1,25(OH)_2D_3$, 1,25-dihydroxyvitamin D_3; OCN, osteocalcin; NI, neonate intestine; ABC, avidin-biotin-peroxidase; BMP, bone morphogenetic protein; CREB, cAMP-response element-binding protein.

enhanced β-catenin levels at early times independently of endogenous TGF-β. These findings raised the possibility that further examination of transcriptional changes occurring as a result of the Smad3 signaling rapidly induced by PTH and enhanced by inhibition of ERK1/2 activity might reveal novel bone anabolic factors.

In the present study, we performed a transcriptome evaluation by DNA microarray analysis of untreated vector alone-transfected (control) and ERK1/2 inhibitor-treated stable Smad3-overexpressing mouse osteoblastic MC3T3-E1 cells and identified a novel bone formation-related factor, Tmem119.

EXPERIMENTAL PROCEDURES

Materials—MC3T3-E1 cells were provided by Dr. H. Kodama (Ohu Dental College, Koriyama, Japan). Mouse calvarial bone cell cultures from 2–4-day ICR mice were obtained from Primary Cell Co., Ltd., Sapporo, Japan. Human PTH-(1–34), human recombinant bone morphogenetic protein-2 (BMP-2), PD98059, phorbol 12-myristate 13-acetate (PMA), forskolin, N^6,$O^{2'}$-dibutyryl cAMP (Bt_2cAMP), H89, 1,25-dihydroxyvitamin D_3 (1,25$(OH)_2D_3$), dexamethasone, human PTH-related protein (PTHrP)-(1–34), anti-β-actin, and anti-FLAG M2 monoclonal antibodies were from Sigma-Aldrich. Anti-Runx2, anti-ALP, anti-osteocalcin (OCN), anti-β-catenin, anti-Smad1, anti-Smad5, anti-phosphorylated Smad2/3, anti-sclerostin, and anti-dentine matrix protein 1 (DMP-1) antibodies were from Santa Cruz Biotechnology (Santa Cruz, CA). SB431542 and anti-Osterix antibody were from Tocris Cookson Ltd. (Bristol, UK) and Abcam Inc. (Cambridge, MA), respectively. The vectors expressing Myc-tagged Smad3 and a mutant, Smad3ΔC, in which the MH2 domain corresponding to amino acid residues 278–425 had been removed, were described previously (9, 10). All other chemicals used were of analytical grade.

Cell Culture—Mouse osteoblastic MC3T3-E1, bone marrow ST2 cells and mouse calvarial bone cells were cultured in α-MEM (containing 50 μg/ml ascorbic acid) with 10% fetal bovine serum (FBS) and 1% penicillin-streptomycin (Invitrogen). Mouse myoblastic C2C12 and African green monkey COS-7 cells were cultured in Dulbecco's modified Eagle's medium (Invitrogen) with 10% FBS and 1% penicillin-streptomycin. The medium was changed twice a week.

Tmem119 Antibody and cDNA—A hexadecapeptide, NH_2-FSEVPDRAPDSRHEEC-COOH, was synthesized (by solid-phase chemistry at the Peptide Synthesis Facility of the Sheldon Biotechnology Centre, McGill University) corresponding to amino acids 145–159 of mouse Tmem119 with an additional cysteine residue at the COOH terminus. The peptide was coupled through the cysteine residue to keyhole limpet hemocyanin, and a rabbit polyclonal antibody was raised by immunization with the conjugate. The antiserum was immunoaffinity-purified before use as described previously (12).

The coding region of mouse Tmem119 was amplified by reverse transcription-PCR of total RNA from MC3T3-E1 cells using 5′-ATAGCTCAACATGGTCCCCTGGTTC-3′ as the forward primer and 5′-GGCCTGTTAGACACTGGGGGA-GAC-3′ as the reverse primer. The cDNA was TA-cloned into the pCR2.1 vector (Invitrogen) according to the manufacturer's specifications. The Tmem119 cDNA insert was cloned into the mammalian expression vector, pcDNA3.1(−) (Invitrogen). The correctness of all constructs was verified by restriction enzyme analysis and nucleotide sequencing.

Transient or Stable Transfection—Each vector was transfected into MC3T3-E1, ST-2, COS-7, or C2C12 cells with Lipofectamine (Invitrogen) as described previously (13–15). Six h later, the cells were fed fresh α-MEM containing 10% FBS. Forty-eight h later, the transiently transfected cells were used for experiments. To generate stably transfected cells, after incubation in α-MEM containing 10% FBS for 48 h, the cells were passaged, and clones were selected in α-MEM supplemented with G418 (0.3 mg/ml; Invitrogen) and 10% FBS. Twenty-four clones were picked after 3 weeks of culture in G418. Several clones were selected after Western blotting with anti-Tmem119 antibody and semiquantitative RT-PCR for Tmem119. To rule out the possibility of clonal variation, at least three independent clones for each stable transfection were characterized. Empty vector-transfected cells were used as control.

Protein Extraction and Western Blot Analysis—Cells were lysed with radioimmunoprecipitation buffer containing 0.5 mM phenylmethylsulfonyl fluoride, complete protease inhibitor mixture (Roche Applied Science), 1% Triton X-100, and 1 mM sodium orthovanadate. Cell lysates were centrifuged at 12,000 × *g* for 20 min at 4 °C, and the supernatants were stored at −80 °C. Protein quantitation was performed with bicinchoninic acid protein assay reagent (Pierce). Twenty-microgram protein aliquots were denatured in SDS sample buffer and separated on 10% polyacrylamide-SDS gels. Proteins were transferred in 25 mM Tris, 192 mM glycine, and 20% methanol to polyvinylidene difluoride. Blots were blocked with 20 mM Tris-HCl (pH 7.5) and 137 mM NaCl plus 0.1% Tween 20 containing 3% dried milk powder. The membranes were immunoblotted with each primary antibody. The antigen-antibody complexes were visualized using the appropriate secondary antibodies (Sigma-Aldrich) and the enhanced chemiluminescence detection system as recommended by the manufacturer (Amersham Biosciences). The results depicted in Figs. 1–8 are representative of at least three separate cell preparations. Each experiment was repeated three times.

RNA Extraction and Semiquantitative RT-PCR—Total RNA was prepared from cells using TRIzol reagent (Invitrogen). Reverse transcription of 5 μg of cultured cell total RNA was carried out for 50 min at 42 °C and then for 15 min at 70 °C using the SuperScript First Strand Synthesis System for RT-PCR (Invitrogen), which contained RT buffer, oligo(deoxythymidine)$_{12-18}$, 5× first-strand solution, 10 mM deoxy-NTP, 0.1 M dithiothreitol, SuperScript II (RT enzyme), and ribonuclease H (ribonuclease inhibitor). PCR, using primers to unique sequences in each cDNA, was carried out in a volume of 10 μl of PCR reaction mixture (supplied by TaKaRa, Otsu, Japan) supplemented with 2.5 units of TaKaRa *Taq*, deoxy-NTP (1.5 mM each), and PCR buffer (10×; 100 mM Tris-HCl (pH 8.3), 500 mM KCl, and 15 mM $MgCl_2$); 25 ng of each primer and 1 μl of template (from a

50-μl RT reaction) were used. Thermal cycling conditions and primer sequences were as follows: 1) initial denaturation at 96 °C for 2 min; 2) cycling for cDNA, specific number of cycles: 96 °C for 1 min, cDNA-specific annealing temperature for 2 min, and 72 °C for 2 min; and 3) final extension at 72 °C for 5 min. Primer sequences, annealing temperature, and cycle numbers were as follows: Tmem119, 5′-TGGTTCCTCCTGTCTCTGCT-3′ and 5′-ATGATCCCTTCCAGGAGGTT-3′ (55 °C; 27 cycles); OASIS (old astrocyte specifically induced substance), 5′-ACCTGGACCACTTTGTGGAG-3′ and 5′-TGGTGTCCTCCATCTTGACA-3′ (55 °C; 27 cycles); 10-day neonate intestine (NI) cDNA, 5′-GCGTTGTGTTGGAACCTTTT-3′ and 5′-GCGCTTACGAAGCGTCTATC-3′ (53 °C; 27 cycles); MGP (matrix-Gla protein); 5′-GAATCTCACGAAAGCAT-3′ and 5′-ACCCGCAGAAGGAAGGA-3′ (49 °C; 20 cycles); osteopontin, 5′-TCACCATTCGGATGAGTCTG-3′ and 5′-ACTTGTGGCTCTGATGTTCC-3′ (55 °C; 28 cycles); ANK, 5′-CTAGCAGGGTTTGTGGGAGAA-3′ and 5′-TTTATGAAGCAGGGGCGTGAA-3′ (56 °C; 23 cycles); GPP-1, 5′-GCCAGGATCAGATGTGGAGATTG-3′ and 5′-TAACCGAGCAGCAGGTCCATAC (63 °C; 32 cycles); and glyceraldehyde-3-phosphate dehydrogenase (GAPDH), 5′-ATCCCATCACCATCTTCCAGGAG-3′ and 5′-CCTGCTTCACCACCTTCTTGATG-3′ (47 °C; 26 cycles). For semiquantitative RT-PCR, the number of cycles was chosen so that amplification remained well within the linear range as assessed by densitometry (National Institutes of Health ImageJ, version 1.08i, public domain program). An equal volume from each PCR was analyzed by 6% nondenaturing PAGE, and ethidium bromide-stained PCR products were evaluated. Marker gene expression was normalized to GAPDH expression in each sample.

Real-time PCR—Total RNA was prepared from cells using TRIzol reagent. cDNA was synthesized using the Superscript™ First-Strand Synthesis System for RT-PCR (Invitrogen). Specific mRNA was quantified by real-time PCR using a 7500 real-time PCR system (Applied Biosystems, Rotkreuz, Switzerland) with SYBR Premix Ex Taq™ II (perfect real-time) kits (TaKaRa) according to the manufacture's standard protocol. The mRNA value for each gene was normalized relative to the mouse GAPDH mRNA levels in RNA samples. Primer sequences were as follows: GAPDH, 5′-GTGTACATGGTTCCAGTATGAGTCC-3′ and 5′-AGTGAGTTGTCATATTTCTCGTGGT-3′; OCN, 5′-CCTGAGTCTGACAAAGCCTTCA-3′ and 5′-GCCGGAGTCTGTTCACTACCTT-3′; and Runx2, 5′-AAATGCCTCCGCTGTTATGAA-3′ and 5′-GCTCCGGCCCACAAATCT-3′.

Small Interfering RNA—Mouse Tmem119 siRNA, mouse Smad3 siRNA, or control siRNA (each from Santa Cruz Biotechnology) were transfected by the procedures recommended by the supplier into cells that were seeded at 5×10^5cells/well using Lipofectamine™ RNAiMAX (Invitrogen).

Microarray Analysis—Total RNA was extracted from stable empty vector (untreated)- or Smad3-transfected, 10 μM PD98059-treated (24 h)-confluent MC3T3-E1 cells using TRIzol reagent. Total RNA was purified using an RNeasy MinElute Cleanup Kit (Qiagen, Tokyo, Japan) to yield an $A_{260/280} > 1.90$. Double-stranded cDNA was synthesized using a T7-oligo(dT) primer with the 3′ IVT Express Kit (Affymetrix Inc., Santa Clara, CA). Hybridization samples were prepared and processed according to the GeneChip Expression Analysis Technical Manual. The Affymetrix murine genome 430 2.0 set was used to compare gene expression. Data were analyzed using GeneChip operating software, version 1.4 (Affymetrix 690036), according to GeneChip Expression Analysis, Data Analysis Fundamentals, part 701190, rev. 4. Using a DNA microarray viewer (Kurabo, Osaka, Japan), the -fold changes in expression between two groups were calculated, log 2-transformed, and further classified as not changed, increased (signal log ratio change p value < 0.005), decreased (signal log ratio change p value < 0.005), or marginally increased or decreased.

Co-immunoprecipitation—For co-immunoprecipitation experiments, cells were lysed with a buffer containing 1% Triton X-100, 1% deoxycholate, 50 mM Tris-HCl (pH 7.4), 100 mM NaCl, 25 mM sodium fluoride, 10 mM sodium pyrophosphate, 2 mM sodium orthovanadate, 1.5 mM $MgCl_2$, and 2 mM EGTA plus protease inhibitor mixture for 30 min at 4 °C; then insoluble materials were separated by centrifugation at 4 °C for 30 min at 15,000 × *g*. An aliquot of the supernatant containing 1 mg of protein was clarified and incubated with anti-FLAG or anti-Runx2 antibody on a rocking platform at 4 °C overnight. The immune complexes were collected with protein G PLUS/protein A-agarose beads (Calbiochem) for 30 min at 4 °C. The beads were washed four times with lysis buffer, resuspended in 2× sample buffer, and boiled for 5 min. Immunoprecipitated proteins were analyzed by SDS-PAGE and subjected to Western blot analysis using anti-Tmem119 antibody as described above.

Luciferase Assay—Cells were seeded at a density of 2×10^5/6-well plate. Twenty-four h later, cells were transfected with 3 μg of reporter plasmid (3GC2 lux or OSC-luci) with the pCH110 plasmid expressing β-galactosidase (1 μg) in each well using Lipofectamine (Invitrogen) as described (15). Fifteen h later, the medium was changed to one containing 4% FBS, and the cells were incubated for an additional 9 h. Thereafter, cells were cultured for 24 h in the presence or absence of 200 ng/ml BMP-2. Cells were lysed, and luciferase activity was measured and normalized to the relative β-galactosidase activity as described (15).

Avidin-biotin-peroxidase (ABC) Complex and Fluorescence Immunocytochemistry—For ABC immunocytochemistry, cells in chamber slides were fixed in 4% paraformaldehyde for 10 min. The slides were incubated in a mixture of 3% H_2O_2 and methanol for 10 min at room temperature to block endogenous peroxidase activity. After treatment with blocking antibody, the primary antibodies were added, and the slides were incubated for 60 min at room temperature. Non-immunized mouse serum was used for preparing negative controls. The ABC method was used with a MaxiTags™ kit (ThermoShandon, Pittsburgh, PA). Final development of the sections was carried out with 3,3′-diaminobenzidine containing 0.03% H_2O_2. For fluorescence immunocytochemistry, after treatment with blocking antibody, the primary antibodies were added and the slides incubated for 60 min at room temperature. The samples were incubated with Cy2-conjugated anti-rabbit IgG (H+L)

TABLE 1
Gene transcripts up-regulated in stably transfected Smad3 MC3T3-E1 cells treated with PD98059 *versus* vector alone-transfected and untreated MC3T3-E1 cells

Gene name	GenBank™ accession No.	Ratio
Genes of known function		
Alp	AW319615	48.5
Bglap1	NM_007541	13.0
C1qtnf3	NM_030888	19.7
Cdsn	BM231053	13.0
Cspg4	BB377873	8.0
Dlx-3	U79738	19.7
Fbxo39	BB645745	5.3
Fzb	U91905	8.0
Gpc1	NM_019738	4.6
Ibsp	NM_008318	137.2
Igfbp-5	BF225802	27.9
Nrp-2	BB409477	11.3
Nupr1	NM_019738	7.0
OASIS	BC016447	7.5
Osterix	NM_130458	17.1
Phf10	NM_024250	4.0
Phospho1	BC004048	157.6
Ptch1	BG071079	9.2
Pthr1	BC013440	147.0
Sdc-3	BB528350	10.6
Smoc2	NM_022315	22.6
Sox-6	AJ010605	73.5
Tcf-7	NM_009331	73.5
Tenascin-C	BB003393	157.6
Tnfrs619	NM_013898	119.4
Tnfrsb11b	AB013898	22.6
Vldlr	NM_013703	17.1
Wif-1	AK017223	315.2
Xpot	AK003432	4.3
Zfp-503	BB447914	8.0
Gene transcripts of unknown function		
Tmem119	BC025600	13.0
NI	5133401	8.0

(Jackson ImmunoResearch, West Grove, PA) for 30 min at room temperature and counterstained with 4′,6-diamidine-2′-phenylindole dihydrochloride (Roche Applied Science).

Statistics—Data are expressed as mean ± S.E. Statistical analysis was performed using analysis of variance. A p value < 0.05 was taken to indicate significant difference.

RESULTS

Transcriptional Profiling—We had demonstrated previously that the PTH-Smad3 axis is involved in the bone anabolic action of PTH in osteoblastic cells including MC3T3-E1 cells (9). Moreover, inhibition of ERK1/2 by PD98059 enhances Smad3-induced bone anabolic action in these cells (8). These findings suggested the hypothesis that examination of the altered Smad3-induced signaling brought about by inhibition of ERK1/2 could identify novel bone anabolic factors in osteoblasts. We therefore performed comparative transcriptional profiling between empty vector stably transfected cells (control) and PD98059-treated Smad3 stably overexpressing MC3T3-E1 cells (experimental) using cDNA microarray analysis. From the ~45,000 genes on the Affymetrix GeneChip, we selected those genes in which expression was increased at least four times in the experimental *versus* the control group. Several known bone-related factors such as ALP, the homeodomain protein Dlx3, fritz b (fzb), insulin-like growth factor-binding protein-5 (IGFBP-5), Phospho1, PTH receptor type 1 (PTHR1), OASIS, Osterix, and tenascin-C were identified (Table 1). In addition, two factors of unknown function (Tmem119 and NI) were identified.

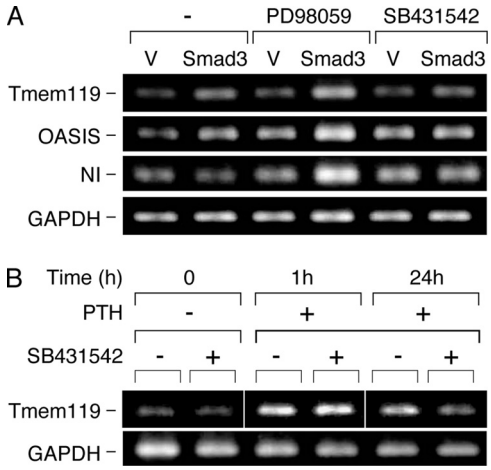

FIGURE 1. **Tmem119 is induced by Smad3 independently of endogenous TGF-β.** *A*, effects of an ERK1/2 inhibitor and a TGF-β inhibitor on mRNA levels of Tmem119, OASIS, and NI in MC3T3-E1 cells overexpressing Smad3. Empty vector (*V*)-transfected or Smad3 (*S*) stably transfected MC3T3-E1 cells were cultured in the presence or absence of 10 μM PD98059 or 3 μM SB431542 for 7 days. Total RNA was extracted, and semiquantitative RT-PCR was performed. *B*, effect of PTH on the level of Tmem119 mRNA in MC3T3-E1 cells. Cells were cultured in the presence or absence of PTH-(1–34) (10^{-8} M) for 0, 1, or 24 h without or with 3 μM SB431542. Total RNA was extracted, and semiquantitative RT-PCR was performed.

Selection of Tmem119—We selected Tmem119 to study further because our previous study had suggested that such a molecule, induced early by PTH but independently of endogenous TGF-β, might be related to the bone anabolic action of PTH (9). Levels of Tmem119 and OASIS mRNA were increased in stably overexpressing Smad3 relative to vector alone-transfected MC3T3-E1 cells by semiquantitative RT-PCR, although the levels of NI mRNA were equivalent in the two types of cells (Fig. 1*A*). The levels of Tmem119, OASIS, and NI RNA were not different in vector alone-expressing cells treated without or with the ERK1/2 inhibitor PD98059. However, the levels of Tmem119, OASIS, and NI mRNA were induced further by treatment of the stably overexpressing Smad3 MC3T3-E1 cells with PD98059 relative to the untreated cells (Fig. 1*A*). Treatment with SB431542, an inhibitor of endogenous TGF-β signaling (activin-like kinase 5 inhibitor), did not alter Smad3 induction of Tmem119 mRNA levels, although it inhibited Smad3 enhancement of OASIS mRNA levels. These findings indicated that of these three factors identified by the microarray analysis only Tmem119 is induced by Smad3 independently of endogenous TGF-β.

PTH elevated the levels of Tmem119 mRNA after both short term (1 h) and long term (24 h) stimulation (Fig. 1*B*). Although the levels of OASIS and NI mRNA were elevated after 24 h of PTH stimulation, at 1 h the levels were unaltered from time 0 (data not shown). Moreover, SB431542 did not antagonize the early induction (at 1 h) of Tmem119 mRNA by PTH, although it antagonized the later induction (at 24 h) of Tmem119 mRNA by PTH (Fig. 1*B*). On the basis of these findings, we selected Tmem119 for further study as a putative bone anabolic factor.

Anti-Tmem119 Antibody and the Expression of Tmem119 in Osteoblastic, Mesenchymal, and Kidney Cells—A rabbit polyclonal antibody against Tmem119 was raised to characterize the expression and function of Tmem119 in osteoblasts and

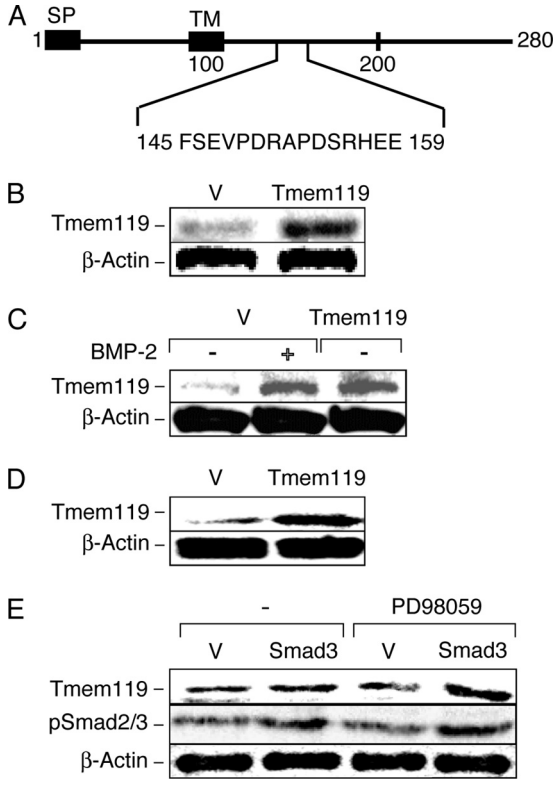

FIGURE 2. **Production of a polyclonal antibody against Tmem119 and Western blot analysis of the protein.** *A*, schematic of mouse Tmem119 showing the locations of the putative signal peptide (*SP*), the transmembrane region (*TM*), and the peptide sequence (amino acids 145–159) against which a rabbit polyclonal antibody was raised. *B*, MC3T3-E1 cells were transfected with 3 μg of empty vector (*V*) or Tmem119 expression vector per well in 6-well plates. After 48 h, protein extraction of the cells and Western blot analysis with anti-Tmem119 and β-actin antibodies were performed. Tmem119 predicted molecular mass is ~30 kDa. *C*, C2C12 cells were transfected with 3 μg of empty vector or Tmem119, and the empty vector cells were treated with or without 200 ng/ml BMP-2 for 48 h. Then protein extraction of the cells and Western blot analysis with anti-Tmem119 and β-actin antibodies were performed. *D*, COS-7 cells were transfected with 3 μg of empty vector or Tmem119 per well in 6-well plates. After 72 h, protein extraction of the cells and Western blot analysis with anti-Tmem119 and β-actin antibodies were performed. *E*, subconfluent empty vector-transfected or Smad3 stably transfected MC3T3-E1 cells were cultured with or without 10 μM PD98059 for 24 h. Then protein extraction of the cells and Western blot analysis with anti-Tmem119, anti-phosphorylated Smad2/3, and β-actin antibodies were performed.

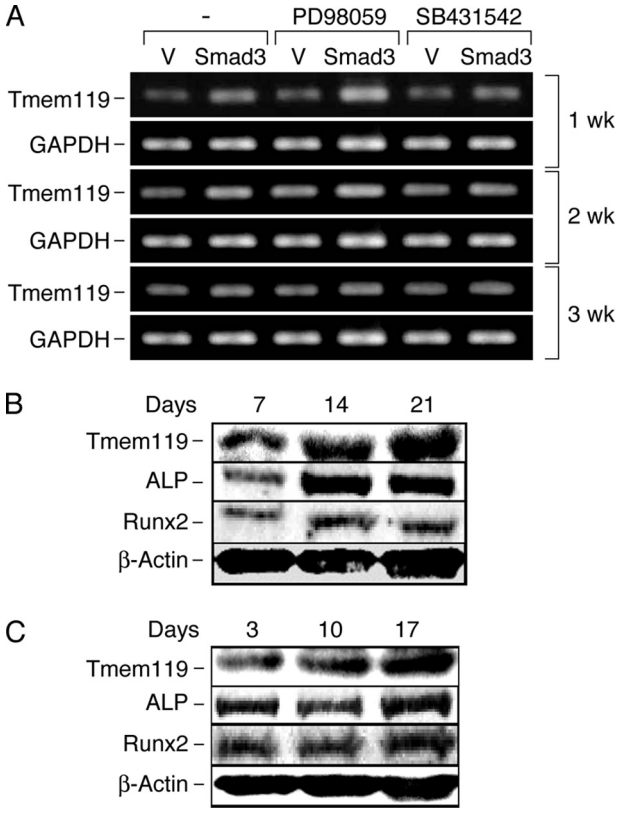

FIGURE 3. **Expression of Tmem119 progressively increases during osteoblast differentiation.** *A*, empty vector (*V*)- or Smad3-transfected MC3T3-E1 cells were cultured in the presence or absence of 10 μM PD98059 or 3 μM SB431542 for 1, 2, and 3 weeks (*wk*). Total RNA was extracted, and semiquantitative RT-PCR for Tmem119 and GAPDH was performed. *B*, wild-type (non-transfected) MC3T3-E1 cells were cultured for 7, 14, and 21 days. Protein extraction of the cells and Western blot analysis with anti-Tmem119, ALP, Runx2, and β-actin antibodies were performed. *C*, ST-2 cells were cultured in the presence of 100 ng/ml BMP-2 for 3, 10, and 17 days. Protein extraction of the cells and Western blot analysis with anti-Tmem119, ALP, Runx2, and β-actin antibodies were performed.

other cells (Fig. 2*A*). By Western blot analysis of the antibody detected the expression of Tmem119 that migrated as a protein of ~30 kDa in MC3T3-E1 cells (Fig. 2*B*). Transient overexpression of Tmem119 elevated the levels of this molecule in these cells. Tmem119 was detected in mouse mesenchymal C2C12 cells, and transient overexpression of Tmem119 elevated the signal (Fig. 2*C*). The addition of BMP-2 increased the level of Tmem119 in these cells (Fig. 2*C*). Moreover, Tmem119 was detected in African green monkey kidney (COS-7) cells, and transient Tmem119 overexpression elevated the level (Fig. 2*D*). The levels of Tmem119 protein were elevated in MC3T3-E1 cells stably overexpressing Smad3, and PD98059 enhanced these protein levels in MC3T3-E1 cells (Fig. 2*E*), showing that the ERK1/2 inhibitor enhances Smad3 induction of Tmem119 at the protein as well as the mRNA level. BMP-2 did not induce the phosphorylation of Smad3 in ST-2 and C2C12 cells in our preliminary study (data not shown).

Tmem119 Expression during Osteoblast Differentiation—MC3T3-E1 cells in culture undergo osteoblastic differentiation with mineralization starting after 2–3 weeks. As we reported previously (14), ALP activity increases with time, and the expression of type 1 collagen and osteopontin peaks at 7 and 14 days of culture, respectively, whereas mRNA expression of OCN, a terminal differentiation marker, is highest at day 21 of culture. The levels of Tmem119 mRNA increased for up to 2 weeks, and the level was maintained up to week 3 in MC3T3-E1 cells (Fig. 3*A*). The effect of PD98059 in augmenting Smad3-induced Tmem119 mRNA expression became less obvious as the culture period progressed and disappeared entirely at day 21. At the protein level, the level of Tmem119 continued to increase during 21 days of culture of the MC3T3-E1 cells (Fig. 3*B*). Mesenchymal ST2 cells differentiate into osteoblastic cells when stimulated with BMP-2, and in cells cultured in this way, the level of Tmem119 increased with time (Fig. 3*C*). Tmem119 levels did not increase in the absence of BMP-2 (data not shown). Therefore, the expression level of Tmem119 correlates with the differentiation stage.

Induction of Tmem119 by PTH—We next examined whether PTH and other osteoblast regulators would affect Tmem119 protein levels in MC3T3-E1 cells. PTH induced the level of

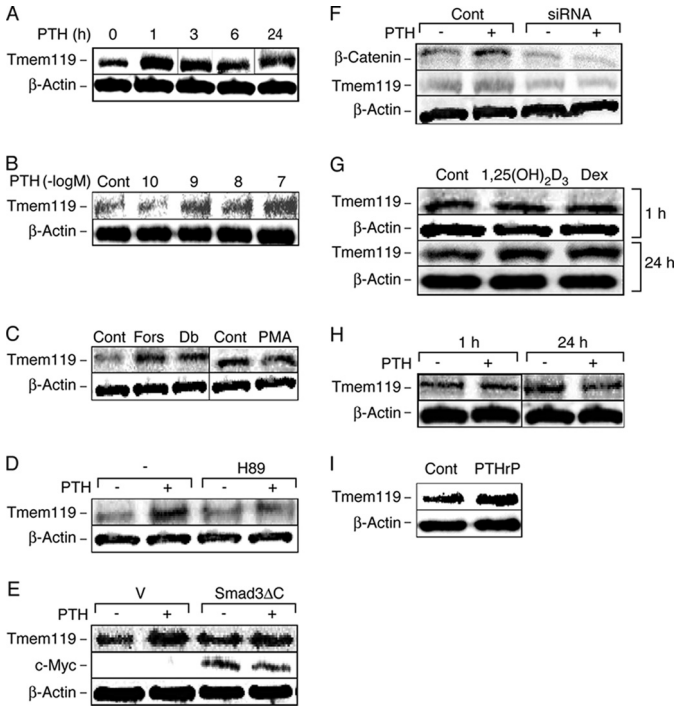

FIGURE 4. **PTH stimulates Tmem119 expression in MC3T3-E1 cells.** Subconfluent MC3T3-E1 cells were treated with 10^{-8} M PTH-(1–34) for the indicated times (*A*) or the indicated concentrations of PTH-(1–34) for 1 h (*B*). Then protein extraction of the cells and Western blot analysis with anti-Tmem119 and β-actin antibodies were performed. *C*, subconfluent MC3T3-E1 cells were treated with 10^{-5} M forskolin (*Fors*), 10^{-4} M Bt_2cAMP (*Db*, dibutyryl cAMP), or 10^{-6} M PMA for 1 h. Then protein extraction of the cells and Western blot analysis with anti-Tmem119 and β-actin antibodies were performed. *D*, subconfluent MC3T3-E1 cells were treated with 10^{-8} M PTH-(1–34) for 1 h in the presence or absence of 10^{-8} M H89. Then protein extraction of the cells and Western blot analysis with anti-Tmem119 and β-actin antibodies were performed. *E*, transiently empty vector (*V*)- or Smad3ΔC-transfected MC3T3-E1 cells that had been treated (+) or not (−) with 10^{-8} M PTH-(1–34) for 1 h were analyzed by Western blot with anti-Tmem119, c-Myc, and β-actin antibodies. *F*, transient control (*Cont*) siRNA- or Tmem119 siRNA-transfected MC3T3-E1 cells that had been treated (+) or not (−) with 10^{-8} M PTH-(1–34) for 1 h were analyzed by Western blot with anti-β-catenin, Tmem119, and β-actin antibodies. *G*, subconfluent MC3T3-E1 cells were treated with 10^{-8} M $1,25(OH)_2D_3$ or 10^{-7} M dexamethasone (*Dex*) for 1 or 24 h. Then protein extraction of the cells and Western blot analysis with anti-Tmem119 and β-actin antibodies were performed. *H*, subconfluent C2C12 cells were treated with 10^{-8} M PTH-(1–34) for 1 or 24 h. Then protein extraction of the cells and Western blot analysis with anti-Tmem119 and β-actin antibodies were performed. *I*, subconfluent MC3T3-E1 cells were treated with 10^{-8} M PTHrP-(1–34) for 1 h. Then protein extraction of the cells and Western blot analysis with anti-Tmem119 and β-actin antibodies were performed.

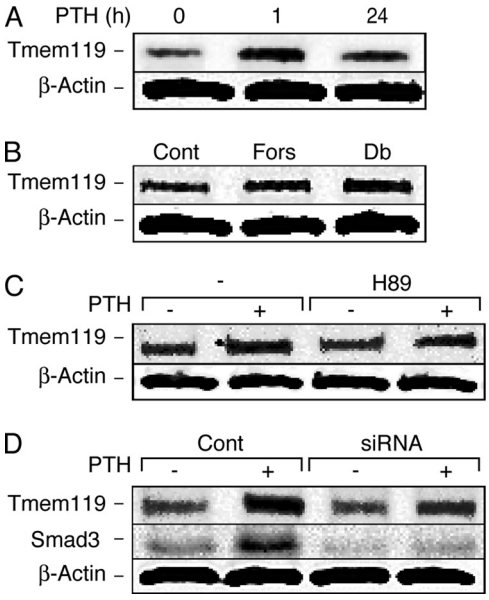

FIGURE 5. **PTH stimulates Tmem119 through Smad3 in mouse primary bone cell cultures.** *A*, subconfluent mouse calvarial bone cells were treated with 10^{-8} M PTH-(1–34) for the indicated times. Then protein extraction of the cells and Western blot analysis with anti-Tmem119 and β-actin antibodies were performed. *B*, subconfluent mouse calvarial bone cells were treated with 10^{-5} M forskolin (*Fors*) or 10^{-4} M Bt_2cAMP (*Db*, dibutyryl cAMP) for 1 h. Then protein extraction of the cells and Western blot analysis with anti-Tmem119 and β-actin antibodies were performed. *C*, subconfluent mouse calvarial bone cells were treated with 10^{-8} M PTH-(1–34) for 1 h in the presence or absence of 10^{-8} M H89. Then protein extraction of the cells and Western blot analysis with anti-Tmem119 and β-actin antibodies were performed. *D*, mouse calvarial bone cells transiently transfected with either control (*Cont*) siRNA or Smad3 siRNA were treated (+) or not (−) with 10^{-8} M PTH-(1–34) for 1 h, and then cell extracts were made and analyzed by Western blot with anti-Smad3, Tmem119, and β-actin antibodies.

Tmem119 protein within 1 h (Fig. 4*A*). The effect was dose-dependent, and a significant increase was observed at 10^{-9} M PTH (Fig. 4*B*). The PKA activators forskolin and Bt_2cAMP induced the levels of Tmem119, but the PKC activator PMA had no effect (Fig. 4*C*). The PKA inhibitor H89 antagonized the PTH stimulation of Tmem119 in these cells (Fig. 4*D*). Inactivation of Smad3 by the dominant negative Smad3ΔC antagonized PTH-induced Tmem119 levels (Fig. 4*E*), indicating that PTH elevates the level of Tmem119 through Smad3 in osteoblasts. Reduction of Tmem119 by siRNA antagonized the level of β-catenin induced by PTH at 1 h in MC3T3-E1 cells (Fig. 4*F*). Moreover, actinomycin D, a transcription inhibitor, antagonized the PTH-induced Tmem119 level at 1 h, although cycloheximide had no effect (data not shown), indicating that PTH rapidly elevates the level of Tmem119 through a transcriptional mechanism but not through new protein synthesis. Neither the active vitamin D metabolite $1,25(OH)_2D_3$ nor the glucocorticoid dexamethasone affected Tmem119 levels under short term (1 h) or longer term (24 h) stimulation (Fig. 4*G*). In contrast to its effect in MC3T3-E1 cells, PTH did not alter Tmem119 protein levels in C2C12 cells (Fig. 4*H*). PTHrP elevated the level of Tmem119 in MC3T3-E1 cells (Fig. 4*I*). These findings suggest that the induction of Tmem119 by PTH is specific for osteoblasts. PTH as well as forskolin and Bt_2cAMP elevated the levels of Tmem119 (Fig. 5, *A* and *B*), and H89 antagonized the PTH stimulation of Tmem119 in mouse primary calvarial cell cultures (Fig. 5*C*). Reduction of Smad3 by siRNA antagonized the level of Tmem119 induced by PTH at 1 h in these cells (Fig. 5*D*).

Immunocytochemistry of Tmem119 Expression—In MC3T3-E1 cell lines stably overexpressing Tmem119, the increased levels of Tmem119 were evident by Western blot analysis (Fig. 6*A*). Next, the cellular expression of Tmem119 was examined in MC3T3-E1 cells by ABC immunocytochemistry using the same antibody. Increased cellular levels of Tmem119 were evident in the stably Tmem119-overexpressing cell lines relative to vector alone-transfected cell lines when examined by immunocytochemistry (Fig. 6*B*). The low level of expression of Tmem119 in unstimulated MC3T3-E1 cells (control) was increased by PTH stimulation at 1 and 24 h (Fig. 6*C*). We performed fluorescence immunocytochemistry in Tmem119 stably overexpressing MC3T3-E1 cells. As shown in Fig. 6*D*, Tmem119 was clearly detected mainly in the cytoplasm. The perinuclear granular

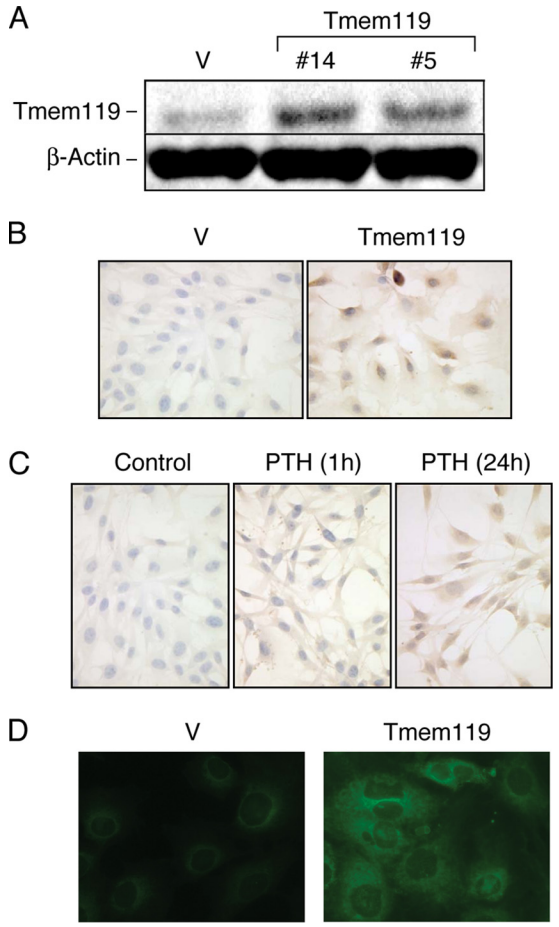

FIGURE 6. **PTH stimulates immunocytochemical Tmem119 expression in MC3T3-E1 cells.** *A*, total protein from empty vector (*V*) stably transfected or Tmem119-transfected MC3T3-E1 (*#5* and *#14*) cells were extracted, and Western blot analysis was performed. *B*, empty vector stably transfected or Tmem119-transfected MC3T3-E1 cells were cultured in chamber slides. Immunocytochemistry for Tmem119 was performed. Representative views of cells are shown. Magnification, ×200. *C*, MC3T3-E1 cells were cultured in chamber slides with or without 10^{-8} M PTH-(1–34) for the indicated times. Immunocytochemistry for Tmem119 was performed. Representative views of cells cultured with or without PTH are shown. Magnification, ×200. *D*, empty vector stably transfected or Tmem119-transfected MC3T3-E1 cells were cultured in chamber slides. Fluorescent immunocytochemistry for Tmem119 was performed. Representative views of cells are shown. Magnification, ×400.

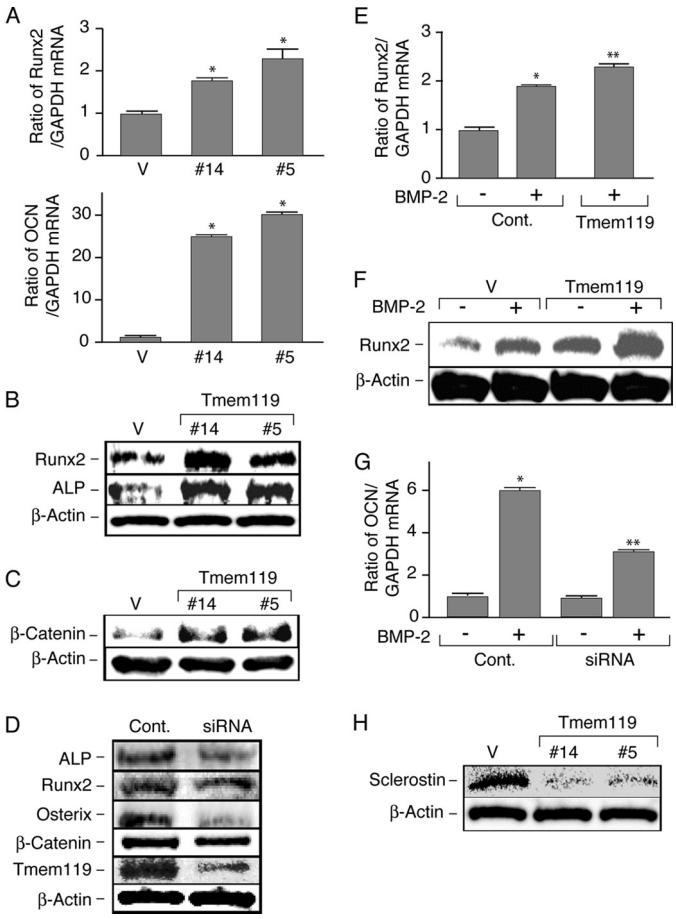

FIGURE 7. **Tmem119 stimulates the differentiation of osteoblasts.** *A*, total RNA from empty vector (*V*) stably transfected or Tmem119-transfected MC3T3-E1 (*#5* and *#14*) cells was extracted, and real-time RT-PCR analysis for Runx2 (*upper panel*), OCN (*lower panel*) and GAPDH was performed. Data were expressed as a ratio of the GAPDH mRNA value. *, significantly different ($p < 0.01$) from the value in empty vector-transfected cells. *B*, total protein from empty vector stably transfected or Tmem119-transfected MC3T3-E1 (*#5* and *#14*) cells was extracted, and Western blot analysis for ALP, Runx2, and β-actin was performed. *C*, total protein from empty vector stably transfected or Tmem119-transfected MC3T3-E1 (*#5* and *#14*) cells was extracted, and Western blot analysis for β-catenin and β-actin was performed. *D*, transient control siRNA- or Tmem119 siRNA-transfected MC3T3-E1 cells were analyzed by Western blot with anti-ALP, Runx2, Osterix, β-catenin, Tmem119, and β-actin antibodies. *E*, ST2 cells with transient transfection of empty vector (*Cont.*) or Tmem119 were cultured in the absence (−) or presence (+) of 200 ng/ml BMP-2 for 48 h. Total RNA was extracted, and real-time RT-PCR analyses for Runx2 and GAPDH were performed. Data are expressed relative to the GAPDH mRNA value. *, significantly different ($p < 0.01$) from the value in empty vector-transfected cells; **, significantly different ($p < 0.05$) from the value in empty vector-transfected and BMP-2-treated cells. *F*, C2C12 cells with transient transfection of vector (*V*) or Tmem119 were cultured in the absence (−) or presence (+) of 300 ng/ml BMP-2 for 48 h. Cell extracts were made, and Western blot analysis for Runx2 and β-actin was performed. *G*, C2C12 cells transfected with control siRNA (*Cont.*) or Tmem119 siRNA (*siRNA*) were treated in the absence (−) or presence (+) of 200 ng/ml BMP-2 for 48 h. Total RNA was extracted, and real-time RT-PCR analyses for OCN and GAPDH were performed. Data are expressed relative to the GAPDH mRNA value. *, significantly different ($p < 0.01$) from the value in control siRNA-transfected cells not treated with BMP-2; **, significantly different ($p < 0.05$) from the value in control siRNA-transfected and BMP-2-treated cells. *H*, total protein from empty vector stably transfected or Tmem119-transfected (*#5* and *#14*) MC3T3-E1 cells was extracted, and Western blot analysis for sclerostin and β-actin was performed.

staining is consistent with location in the endoplasmic reticulum.

Tmem119 Promotes Osteoblast Differentiation—We examined the relationship between Tmem119 expression and osteoblast differentiation in MC3T3-E1 cells stably overexpressing Tmem119 *versus* vector alone-expressing MC3T3-E1 cells. The mRNA and protein levels of the key osteoblast differentiation markers Runx2 and OCN were elevated in the Tmem119-overexpressing cells (Fig. 7, *A* and *B*). The protein levels of ALP, an osteoblast differentiation marker (Fig. 7*B*), and β-catenin, a critical regulator of the osteoblast (Fig. 7*C*), were also elevated in the Tmem119-overexpressing cells. In our preliminary study, the enhancement of Tmem119 overexpression on osteoblast differentiation markers such as ALP and Runx2 levels increased from culture day 7 until day 14 and then seemed to decrease at day 21 in MC3T3-E1 cells (data not shown). A reduction in Tmem119 level by siRNA suppressed the level of ALP, Runx2, Osterix, and β-catenin in MC3T3-E1 cells (Fig. 7*D*).

In addition, we evaluated the role of Tmem119 in mesenchymal cells using transient overexpression of Tmem119 in ST-2

and C2C12 cells. The BMP-2-induced Runx2 mRNA levels were higher in the Tmem119 *versus* vector alone-transfected ST-2 cells (Fig. 7*E*). Moreover, the basal levels and the BMP-2-stimulated levels of Runx2 protein were increased in Tmem119 relative to vector alone, transiently transfected C2C12 cells (Fig. 7*F*). A reduction in Tmem119 by siRNA antagonized the level of OCN mRNA induced by BMP-2 in C2C12 cells (Fig. 7*G*). In our preliminary data, stable overexpression of Tmem119 did not affect the levels of GPP-1, ANK, and osteopontin mRNA in semiquantitative-RT-PCR in MC3T3-E1 cells. Moreover, Tmem119 overexpression did not affect the levels of DMP-1 (data not shown). However, it suppressed the level of sclerostin in these cells (Fig. 7*H*).

Interaction between Tmem119 and Smad1/5 or Runx2—Finally, we examined the physical interactions between Tmem119 and BMP-specific Smads, Smad1 and Smad5, and Runx2 in C2C12 and MC3T3-E1 cells. Tmem119 coimmunoprecipitated with Smads 1 and 5 and Runx2 in C2C12 cells (Fig. 8, *A–C*). PTH rapidly enhanced the coimmunoprecipitation of Tmem119 and Smad5 or Runx2 in MC3T3-E1 cells (Fig. 8*D*). Reduction of Tmem119 by siRNA significantly antagonized Runx2-induced transcriptional activity as well as BMP-2- and Smad5-induced transcriptional activity in C2C12 cells (Fig. 8, *E* and *F*). All data are from experiments repeated three times with reproducible results.

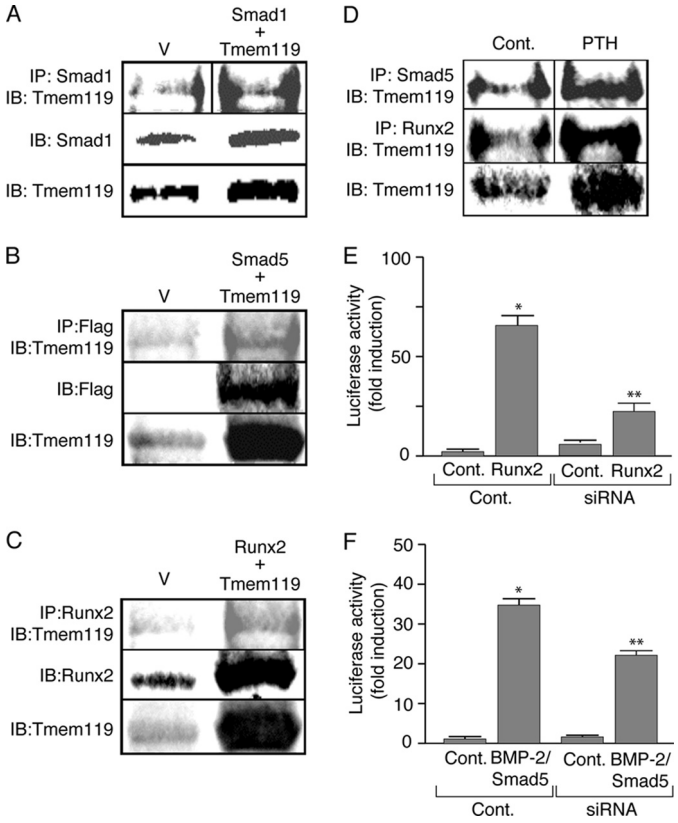

FIGURE 8. **Tmem119 coimmunoprecipitates with Smad1, Smad5, and Runx2 in mesenchymal stem cells.** C2C12 cells were transfected with vector only (*V*) or Tmem119 with Smad1 (*A*), FLAG-tagged Smad5 (*B*), or Runx2 (*C*). Forty-eight h later, cell extracts were made and immunoprecipitated (*IP*) with anti-Smad1 (*A*), anti-FLAG (*B*), or anti-Runx2 (*C*) antibodies followed by immunoblotting (*IB*) with anti-Smad1 antibody (*A*), anti-FLAG antibody (*B*), or anti-Runx2 antibody (*C*) and anti-Tmem119 antibody (*A–C*). *D*, subconfluent MC3T3-E1 were cultured with or without PTH-(1–34) for 1 h. Cell extracts were made and immunoprecipitated with anti-Smad5 or Runx2 antibodies followed by immunoblotting with anti-Tmem119 antibody. *E*, the Runx2 promoter-reporter construct, OSC-luci, was transfected with vector or Runx2 into C2C12 cells that had been transfected 24 h earlier with either control (*Cont.*) or Tmem119 siRNA. Relative luciferase activity was measured as described under "Experimental Procedures." Each value is the mean ± S.E. of four determinations. *, $p < 0.01$, compared with vector only-transfected group; **, $p < 0.01$, compared with Runx2- and control siRNA-transfected group. *F*, C2C12 cells were transfected with either control or Tmem119 siRNA; 24 h later they were transfected with the Smad1/5 reporter construct (3GC2-lux), with vector only, or with Smad5 and treated (+) or not (−) with 200 ng/ml BMP-2. Relative luciferase activity was measured as described under "Experimental Procedures." Each value is the mean ± S.E. of four determinations. *, $p < 0.01$, compared with the vector only-transfected group. **, $p < 0.01$, compared with the Smad5- and control siRNA-transfected group.

DISCUSSION

Multipotential mesenchymal stem cells, derived from mesoderm, become osteoprogenitors and commit to the osteoblast lineage. Thereafter, the cells undergo further differentiation, exhibiting an osteoblast-specific phenotype, and express ALP and OCN. Concomitant with the osteoblast maturation process, extracellular matrix is mineralized or calcified, and bone is formed. These sequential events are regulated by hormones such as PTH and cytokines such as TGF-β. The intracellular signaling pathways triggered by these factors cross-talk to each other forming a complex network. These signaling pathways drive the activities of transcriptional factors such as Runx2, which are critical for osteoblast differentiation (16–20).

Several known important bone-related factors were identified by the gene profiling in osteoblastic MC3T3-E1 cells that specifically searched for genes that are up-regulated by increased Smad3 expression in the presence of an ERK1/2 inhibitor. Among them, Dlx3, Fzb, IGFBP-5, Phospho1, PTHR1, OASIS, Osterix, and tenascin-C can be noted. Dlx3 is a homeodomain protein induced by BMP-2 that activates Runx2 gene transcription and is critical for the commitment of mesenchymal stem cells to the osteogenic lineage (21). The frizzled-related protein, Fzb, modulates Wnt-β-catenin signaling, important for bone formation (22). IGFBP-5 is related to osteoblast proliferation and differentiation, both dependently on and independently of IGF-1 action (23). OASIS, a member of the CREB/ATF transcription factor family with a transmembrane domain, is highly expressed in osteoblasts (24) and undergoes regulated intramembrane proteolysis in response to endoplasmic reticulum stress inducing *Col1a1* gene transcription (25). Osterix is essential for osteoblastic bone formation downstream of Runx2 (26). Phospho1 is involved in mineralization (27), and tenascin-C is a bone matrix protein (28). Therefore, these important factors may function downstream of Smad3 in osteoblastic bone formation.

The Tmem119 transcript identified here as encoding an important bone-related factor came to attention previously as a differentially regulated transcript (of unknown function) in a comparative study of the expression profiles of E14.5 wild-type and *Runx2*$^{-/-}$ mouse embryonal humerii assessed by microarray analysis (29). Expression of Tmem119 was detected in the perichondrium, the trabecular bone, and the stratum osteogenicum in the periosteum but not in chondrocytes and osteoclasts. The transcript levels are increased in differentiated calvarial cultures (day 17) with increased expression in cells sorted for *Col1a1* promoter activity (30) (NCBI DataSet record GDS1632).

Mouse Tmem119 has 280 amino acids (molecular mass, 29,401 Da) and human Tmem119 has 283 amino acids (29,072 Da). The mouse and human proteins share 75% similarity and 70% identity and are encoded by genes on syntenic loci at mouse chromosome 5 and human 12q24.11, respectively. Tmem119 is predicted to be a single-pass type 1a membrane protein with amino acids 113–280 (in the mouse) comprising a cytoplasmic tail. Consistent with its being a type 1a membrane protein (and hence having a cleavable signal peptide), Tmem119 is predicted to have a signal peptide (which directs the nascent polypeptide to the endoplasmic reticulum) of ~18 amino acids (PSORT and SignalP) with residues 90–112 (TMHMM method) comprising the transmembrane helix. By expressed sequence tag (EST) profiling, Tmem119 mRNA is expressed in several tissues including blood, bone, brain, intestine, kidney, liver, lung, skin, and uterus but apparently not in adipose, bladder, heart, lymph node, muscle, ovary, testis, pancreas, spleen, and spinal cord in mice (UGID: 270244; UniGene Mm.41681).

The present studies show that the expression levels of Tmem119 correlate with the differentiation (commitment) of mesenchymal stem cells into the osteoblast lineage and differentiation of preosteoblasts to osteoblasts with enhanced expression of the differentiation markers Runx2, ALP, OCN, and β-catenin. Although Runx2 is critical for the commitment of mesenchymal stem cells into the osteoblast lineage (16, 31–33), transgenic mice overexpressing Runx2 under the control of the osteoblast-specific *Col1a1* promoter exhibit decreased bone mineralization and increased bone resorption (34). Although in the Runx2 osteoblast-overexpressing transgenic mice, the osteoblast number is increased at an early differentiation stage, osteoblast functions (matrix production and mineralization) were impaired in these cells (34). Thus, Runx2 inhibits later osteoblast differentiation, in contrast to its positive action on early osteoblast development, whereas Tmem119 induces both the early and late stages of osteoblast differentiation.

PTH specifically and dose-dependently induced Tmem119 in osteoblastic cells but not in mesenchymal stem cells. The response occurred via the PKA but not the PKC pathway within 1 h. (Other osteoblast regulators like $1,25(OH)_2D_3$ and glucocorticoids were without effect even after 24 h of stimulation.) The roles of the PKA- and PKC-signaling pathways in bone formation are controversial. Some studies have found that PTH exerts anti-apoptotic actions in osteoblasts through PKA signaling (35, 36). Others have reported that intermittent treatment with PTH stimulates bone anabolism through both PKA and PKC pathways in osteoblasts (37). However, it has been reported that PKC activity inhibits osteoblast differentiation (38). In the present study, forskolin and Bt_2cAMP induced the level of Tmem119 in osteoblasts, although PMA, a PKC activator, was without effect. Moreover, a PKA inhibitor antagonized the PTH-induced effects. Hence, these findings indicate that PTH induces Tmem119 through the cAMP pathway.

Our previous studies indicated that PTH rapidly elevates the level of β-catenin through Smad3 in osteoblasts (9–11). In the present study, inactivation of Smad3 antagonized the induction of Tmem119 levels by PTH, and reduction of Tmem119 levels antagonized the induction of β-catenin by PTH in osteoblasts These findings indicate that PTH elevates Tmem119 levels through Smad3, resulting in an elevation in β-catenin, which might lead to bone anabolic effects.

By immunocytochemistry, Tmem119 was detected in MC3T3-E1 cells, and increased levels of expression were observed after stimulation of the cells for 1 or 24 h with PTH. Clear perinuclear staining was observed consistent with location in the endoplasmic reticulum membrane, with the COOH-terminal part (which contains the epitope recognized by the antibody) being cytoplasmic. Further studies will be required to identify the precise cellular location of Tmem119 under different conditions. However, the putative function of Tmem119 might be surmised to be different from that of another transmembrane protein highly expressed in the osteoblast, namely OASIS. OASIS is an endoplasmic reticulum stress transducer. This type 2 membrane protein, without a cleavable signal peptide and oriented in the opposite direction to a type 1 membrane protein (in contrast to Tmem119), is a member of the CREB/ATF transcription factor family (24). In response to endoplasmic reticulum stress, OASIS trafficks to the Golgi where it undergoes intramembrane cleavage, and the released bZip motif-containing NH_2-terminal part enters the nucleus inducing *Col1a1* gene transcription (25). In contrast to OASIS, Tmem119 has no endoplasmic reticulum retention motifs, nuclear localization sequences, or transcriptional regulator motifs.

The BMP-Runx2 pathway is critical for bone formation (39, 40). The transcription factors Runx2 and Smad1/5 that are involved in this pathway exist in the cytoplasm as well as the nucleus. We showed that Tmem119 is complexed with Smad1/5 and Runx2 in C2C12 cells. Moreover, a reduction in Tmem119 antagonized Runx2- or Smad5-mediated transcriptional activity. Also, the levels of Tmem119 increased with time in these pluripotent cells treated with BMP-2 and undergoing commitment to the osteoblast lineage. Increased levels of Tmem119 induced the expression of osteoblast differentiation markers. Together these findings suggest that Tmem119 induces the commitment of multipotential mesenchymal cells to become osteoblasts through a mechanism involving the BMP-2-Smad1/5-Runx2 cascade.

In the present study, stable Tmem119 overexpression reduced the level of sclerostin in MC3T3-E1 cells. A constitutive overexpression of Tmem119 at developmentally inappropriate time points might lead to an inhibition of osteocyte differentiation. Alternatively, a recent study has indicated that the suppression of sclerostin expression contributes to the bone anabolic action of intermittent PTH treatment in mice (41). Therefore, reduction of the sclerostin level by Tmem119 might be related to the bone anabolic action of PTH.

While this manuscript was in preparation, Kanamoto *et al.* (42) reported on Tmem119 as a predominantly expressed gene in osteoblasts, based on microarray screening using a mouse chondroprogenitor cell line, ATDC5. Consistent with our data, Tmem119 stimulated differentiation in osteoblasts (42). Moreover, overexpression and knockdown enhanced and suppressed mineralization in MC3T3-E1 cells, respectively (42).

Taken together, Tmem119 is an important osteoblast differentiation factor.

In conclusion, we have identified Tmem119 as a novel Smad3-related factor in osteoblastic cells. PTH induces Tmem119 through the cAMP-PKA pathway, and Tmem119 induces osteoblast differentiation. The precise mechanism whereby Tmem119 influences osteoblast biology remains to be elucidated.

Acknowledgments—We thank Y. Higashimaki and E. Matsumoto for technical expertise, Drs. K. Miyazono, J. J. Lebrun, and Y. Chen for plasmids, and Dr. Monzur Murshed for critical review of the manuscript.

REFERENCES

1. Hodsman, A. B., Bauer, D. C., Dempster, D. W., Dian, L., Hanley, D. A., Harris, S. T., Kendler, D. L., McClung, M. R., Miller, P. D., Olszynski, W. P., Orwoll, E., and Yuen, C. K. (2005) *Endocr. Rev.* **26,** 688–703
2. Rosen, C. J., and Bilezikian, J. P. (2001) *J. Clin. Endocrinol. Metab.* **86,** 957–964
3. Swarthout, J. T., D'Alonzo, R. C., Selvamurugan, N., and Partridge, N. C. (2002) *Gene* **282,** 1–17
4. Dempster, D. W., Cosman, F., Parisien, M., Shen, V., and Lindsay, R. (1993) *Endocr. Rev.* **14,** 690–709
5. Kaji, H., Naito, J., Sowa, H., Sugimoto, T., and Chihara, K. (2006) *Horm. Metab. Res.* **38,** 740–745
6. Sowa, H., Kaji, H., Yamaguchi, T., Sugimoto, T., and Chihara, K. (2002) *J. Bone Miner. Res.* **17,** 1190–1199
7. Borton, A. J., Frederick, J. P., Datto, M. B., Wang, X. F., and Weinstein, R. S. (2001) *J. Bone Miner. Res.* **16,** 1754–1764
8. Sowa, H., Kaji, H., Yamaguchi, T., Sugimoto, T., and Chihara, K. (2002) *J. Biol. Chem.* **277,** 36024–36031
9. Sowa, H., Kaji, H., Iu, M. F., Tsukamoto, T., Sugimoto, T., and Chihara, K. (2003) *J. Biol. Chem.* **278,** 52240–52252
10. Tobimatsu, T., Kaji, H., Sowa, H., Naito, J., Canaff, L., Hendy, G. N., Sugimoto, T., and Chihara, K. (2006) *Endocrinology* **147,** 2583–2590
11. Inoue, Y., Canaff, L., Hendy, G. N., Hisa, I., Sugimoto, T., Chihara, K., and Kaji, H. (2009) *J. Cell. Biochem.* **108,** 285–294
12. Kaji, H., Canaff, L., Goltzman, D., and Hendy, G. N. (1999) *Cancer Res.* **59,** 5097–5101
13. Kaji, H., Canaff, L., Lebrun, J. J., Goltzman, D., and Hendy, G. N. (2001) *Proc. Natl. Acad. Sci. U.S.A.* **98,** 3837–3842
14. Sowa, H., Kaji, H., Canaff, L., Hendy, G. N., Tsukamoto, T., Yamaguchi, T., Miyazono, K., Sugimoto, T., and Chihara, K. (2003) *J. Biol. Chem.* **278,** 21058–21069
15. Sowa, H., Kaji, H., Hendy, G. N., Canaff, L., Komori, T., Sugimoto, T., and Chihara, K. (2004) *J. Biol. Chem.* **279,** 40267–40275
16. Ducy, P., Zhang, R., Geoffroy, V., Ridall, A. L., and Karsenty, G. (1997) *Cell* **89,** 747–754
17. Komori, T., Yagi, H., Nomura, S., Yamaguchi, A., Sasaki, K., Deguchi, K., Shimizu, Y., Bronson, R. T., Gao, Y. H., Inada, M., Sato, M., Okamoto, R., Kitamura, Y., Yoshiki, S., and Kishimoto, T. (1997) *Cell* **89,** 755–764
18. Otto, F., Thornell, A. P., Crompton, T., Denzel, A., Gilmour, K. C., Rosewell, I. R., Stamp, G. W., Beddington, R. S., Mundlos, S., Olsen, B. R., Selby, P. B., and Owen, M. J. (1997) *Cell* **89,** 765–771
19. Mundlos, S., Otto, F., Mundlos, C., Mulliken, J. B., Aylsworth, A. S., Albright, S., Lindhout, D., Cole, W. G., Henn, W., Knoll, J. H., Owen, M. J., Mertelsmann, R., Zabel, B. U., and Olsen, B. R. (1997) *Cell* **89,** 773–779
20. Komori, T. (2002) *J. Cell. Biochem.* **87,** 1–8
21. Hassan, M. Q., Tare, R. S., Lee, S. H., Mandeville, M., Morasso, M. I., Javed, A., van Wijnen, A. J., Stein, J. L., Stein, G. S., and Lian, J. B. (2006) *J. Biol. Chem.* **281,** 40515–40526
22. Westendorf, J. J., Kahler, R. A., and Schroeder, T. M. (2004) *Gene* **341,** 19–39
23. Rajaram, S., Baylink, D. J., and Mohan, S. (1997) *Endocr. Rev.* **18,** 801–831
24. Nikaido, T., Yokoya, S., Mori, T., Hagino, S., Iseki, K., Zhang, Y., Takeuchi, M., Takaki, H., Kikuchi, S., and Wanaka, A. (2001) *Histochem. Cell. Biochem.* **116,** 141–148
25. Murakami, T., Saito, A., Hino, S., Kondo, S., Kanemoto, S., Chihara, K., Sekiya, H., Tsumagari, K., Ochiai, K., Yoshinaga, K., Saitoh, M., Nishimura, R., Yoneda, T., Kou, I., Furuichi, T., Ikegawa, S., Ikawa, M., Okabe, M., Wanaka, A., and Imaizumi, K. (2009) *Nat. Cell Biol.* **11,** 1205–1211
26. Nakashima, K., Zhou, X., Kunkel, G., Zhang, Z., Deng, J. M., Behringer, R. R., and de Crombrugghe, B. (2002) *Cell* **108,** 17–29
27. Roberts, S., Narisawa, S., Harmey, D., Millán, J. L., and Farquharson, C. (2007) *J. Bone Miner. Res.* **22,** 617–627
28. Alford, A. I., and Hankenson, K. D. (2006) *Bone* **38,** 749–757
29. Hecht, J., Seitz, V., Urban, M., Wagner, F., Robinson, P. N., Stiege, A., Dieterich, C., Kornak, U., Wilkening, U., Brieske, N., Zwingman, C., Kidess, A., Stricker, S., and Mundlos, S. (2007) *Gene Expr. Patterns* **7,** 102–112
30. Kalajzic, I., Staal, A., Yang, W. P., Wu, Y., Johnson, S. E., Feyen, J. H., Krueger, W., Maye, P., Yu, F., Zhao, Y., Kuo, L., Gupta, R. R., Achenie, L. E., Wang, H. W., Shin, D. G., and Rowe, D. W. (2005) *J. Biol. Chem.* **280,** 24618–24626
31. Krishnan, V., Moore, T. L., Ma, Y. L., Helvering, L. M., Frolik, C. A., Valasek, K. M., Ducy, P., and Geiser, A. G. (2003) *Mol. Endocrinol.* **17,** 423–435
32. D'Alonzo, R. C., Kowalski, A. J., Denhardt, D. T., Nickols, G. A., and Partridge, N. C. (2002) *J. Biol. Chem.* **277,** 24788–24798
33. Stein, G. S., Lian, J. B., van Wijnen, A. J., Stein, J. L., Montecino, M., Javed, A., Zaidi, S. K., Young, D. W., Choi, J. Y., and Pockwinse, S. M. (2004) *Oncogene* **23,** 4315–4329
34. Liu, W., Toyosawa, S., Furuichi, T., Kanatani, N., Yoshida, C., Liu, Y., Himeno, M., Narai, S., Yamaguchi, A., and Komori, T. (2001) *J. Cell Biol.* **155,** 157–166
35. Jilka, R. L., Weinstein, R. S., Bellido, T., Roberson, P., Parfitt, A. M., and Manolagas, S. C. (1999) *J. Clin. Invest.* **104,** 439–446
36. Bellido, T., Ali, A. A., Plotkin, L. I., Fu, Q., Gubrij, I., Roberson, P. K., Weinstein, R. S., O'Brien, C. A., Manolagas, S. C., and Jilka, R. L. (2003) *J. Biol. Chem.* **278,** 50259–50272
37. Ishizuya, T., Yokose, S., Hori, M., Noda, T., Suda, T., Yoshiki, S., and Yamaguchi, A. (1997) *J. Clin. Invest.* **99,** 2961–2970
38. Ogata, N., Kawaguchi, H., Chung, U. I., Roth, S. I., and Segre, G. V. (2007) *J. Biol. Chem.* **282,** 35757–35764
39. Yamaguchi, A., Komori, T., and Suda, T. (2000) *Endocr. Rev.* **21,** 393–411
40. Lee, K. S., Kim, H. J., Li, Q. L., Chi, X. Z., Ueta, C., Komori, T., Wozney, J. M., Kim, E. G., Choi, J. Y., Ryoo, H. M., and Bae, S. C. (2000) *Mol. Cell. Biol.* **20,** 8783–8792
41. Kramer, I., Loots, G. G., Studer, A., Keller, H., and Kneissel, M. (2010) *J. Bone Miner. Res.* **25,** 178–189
42. Kanamoto, T., Mizuhashi, K., Terada, K., Minami, T., Yoshikawa, H., and Furukawa, T. (2009) *BMC Dev. Biol.* **9,** 70